Chapter 6
Land Surface: Coupled Footprints

Coupling footprint models to datasets characterizing surface properties is a most useful endeavour when surface-exchange information is sought (fluxes or parameters characterizing a surface of interest). Land-cover maps are particularly helpful in that regard to identify the various land-cover types contributing to the footprint area. Footprint models require information on characteristics of the underlying surface for surface-related properties needed in footprint calculations such as roughness length. Often, area-averaging methods are necessary to determine the input parameters for the model (see Sect. 2.4). In this chapter, principles underpinning the coupling of footprint models are described. The application of the described methods is given in Chap. 8.

6.1 Grid Schema of Surface Characteristics

Coupling footprint model runs with data describing surface characteristics around a measurement site requires dividing the surrounding landscape into discrete matrices (Fig. 6.1). In these matrices, each grid cell contains mean attributes of the area it represents, such as an integer ID that indicates most land cover classes, or values for e.g. averaged roughness length or stand height. The required spatially explicit information can best be prepared using typical Geographical Information System (GIS) software. Alternatively, the matrices can be produced using maps describing e.g. the land-cover structure in the domain.

The dimensions of the model domain must be sufficiently large to enclose large footprint areas in stable night time conditions, while the grid resolution has to be sufficiently high to yield plausible results in convective, unstable conditions with associated small footprints. The local wind climatology should be taken into

M. Y. Leclerc and T. Foken, *Footprints in Micrometeorology and Ecology*,
DOI: 10.1007/978-3-642-54545-0_6, © Springer-Verlag Berlin Heidelberg 2014

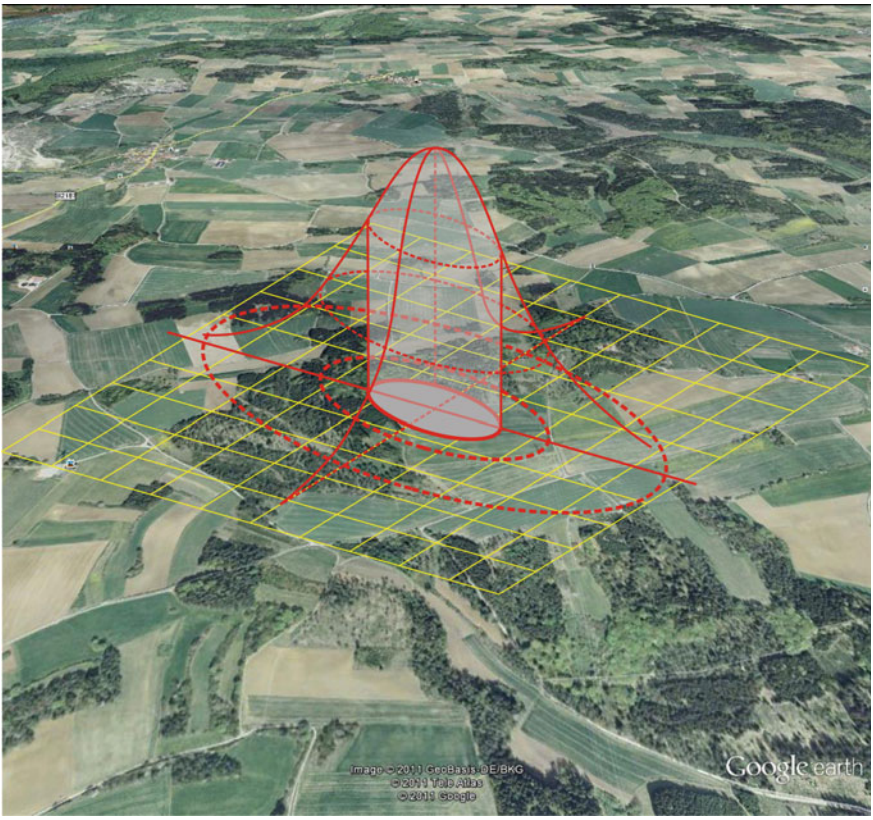

Fig. 6.1 Map with grid elements covering the possible footprint area and the effect levels in upwind direction from the measuring point at the right side (Published with kind permission of © 2011 GeoBasis DE/BKG © 2011 Tele Atlas © 2011 Google. All Rights Reserved)

consideration to reduce processing time in both preparation steps—the creation of land use maps and footprint simulations. Final settings should be tested with preliminary model runs based on different input parameters. It is generally recommended to reduce the size of the grid elements, since higher resolution enables a realistic representation of smaller scale heterogeneities throughout the model domain, avoiding the application of complex averaging schemes.

Over heterogeneous terrain, land-cover information is important to control and investigate the influence of the underlying surface in the footprint of micrometeorological measurements. Regarding distinguished land cover classes, the scheme to be chosen needs to be customized for the specific objective of each footprint study. Many FLUXNET observation sites target to monitor carbon exchange processes for a specific land-cover type, e.g. mixed forest, so in the simplest case a land-cover map is required that differentiates this target (forest) from other areas (non-forest). This approach can be refined into arbitrary levels of details such as differentiating coniferous from deciduous forests, or dividing one forest type into

Table 6.1 List of land cover classes for the preparation of a land use matrix from topographical map information

Surface	Comment
Forest	If the forest is the target area, the major forest types should be accounted for deciduous, coniferous, mixed and given their own respective class. In addition, it is recommended to separate forest sections with different roughness characteristics (age classes, height)
Settlement	Rural settlements, buildings
Traffic areas	Roads
Water areas	Lakes, rivers
Grassland	Permanent grassland, pasture land
Agricultural areas	Crops of all kind. When possible, several classes should be identified according to their respective roughness and thermal characteristics

age classes. Since different land cover classes are often also associated with different roughness lengths which have an impact on the local flow characteristics and therefore on footprint computation, it is recommended to describe the surrounding landscape as accurately as possible. However, at the bare minimum, land-cover classes listed in Table 6.1 should be distinguished.

Since the size and position of the footprint area changes with wind direction, measurement height and atmospheric stability, these factors must be taken into account when setting up the domain for a specific footprint study. As a general guideline, suitable matrix sizes are 5×5 km^2 for tower measurements over tall forests and 0.5×0.5 km^2 for experiments (sensor height approximately 2–3 m) over agricultural areas. Concerning the matrix resolution, information should be provided for grid elements of 25×25 m^2 or smaller, as typically provided by remote sensing data sources such as Landsat. Besides the benefit of representing small scale heterogeneities adequately, such high resolution matrices are necessary to project the source weight function onto the grid, particularly in the case of smaller footprints in unstable conditions.

When remote sensing data is available, the creation of large model domains with high resolution grids as outlined above should be easily achieved; however, such high-resolution settings are impractical in the case where matrices have to be produced from conventional data such as e.g. topographic maps. In addition, computational demand related to both processing time and memory requirements scale with the total number of grid cells in the model domain, thus an optimized domain setup can help increasing the efficiency of the data processing. Figure 6.2 provides a guideline on customizing the domain size and resolution, based on sensor height.

Concerning the dimensions of the area to be covered by the model domain, the parameter D_{min} defines the minimum fetch in each direction (Fig. 6.2). For example, if D_{min} has a value of 1 km, the resulting minimum-matrix would be a square of 2×2 km^2, with the tower located at the center of the area. The second parameter D_{ext} defines an extended fetch distance into the main wind direction. The parameter L_R gives the required resolution for the given matrix size. The minimum settings for D_{min}, D_{ext}, and L_R for specific ranges of the effective

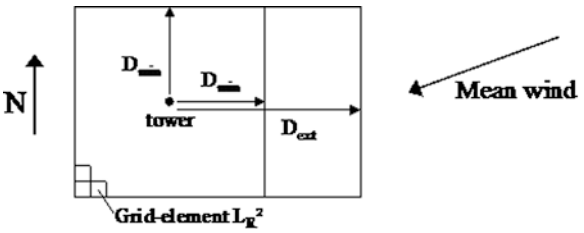

Fig. 6.2 Sketches of the concept of the matrix dimensions defined by parameters D_{min}, D_{ext} and L_R with a stream wisest direction of East-North-East

Table 6.2 Parameter selection for D_{min}, D_{ext}, and L_R (see Fig. 6.2) for the effective measurement height $z_{m\text{-}eff}$

$z_{m\text{-}eff}$ (m)	D_{min} (m)	D_{ext} (m)	L_R (m)
<4	600	1,000	50
4–7	1,200	1,600	80
7–10	1,400	2,000	100
10–13	1,400	2,200	100
13–16	1,500	2,400	100
16–20	1,800	3,300	150
20–24	2,100	3,300	150
>24	2,400	3,600	150

measurement height $z_{m\text{-}eff}$, typically the height above zero-plane displacement, are given in Table 6.2. A map covering a larger domain, or with a higher resolution, will further enhance the accuracy of the footprint approach in the stable as well as in the convective case.

6.2 Determination of Surface Characteristics

The key surface properties to account for in eddy-covariance footprint computation are the land-cover types. That parameter is required to incorporate the contribution of the designated target vegetation to the footprint. Since land-cover types impact the roughness length, one can see the importance of such an input parameter in footprint models. It is thus essential to characterize different land-cover types with individual roughness length values (Sect. 6.2.1). Furthermore, a methodology to determine the land-cover structure either through topographic maps or remote sensing techniques is needed (Sect. 6.2.2). Finally, the determination of other area averaged input data for footprint models is discussed (Sect. 6.3).

6.2.1 Roughness Length

The quality and success of analyses aiming at identifying the contribution of upwind sources to a point area hinges to a large degree to the judicious choice of

Fig. 6.3 The typical landscape in Southwest England with rows of bushes or stones against wind erosion shows that not the roughness of the single fields but the combined roughness of the structured landscape with of fields and bushes creates the effective roughness of the landscape (*Photograph* by Foken)

an appropriate roughness length classification. This is most easily accomplished using an effective roughness length (Fiedler and Panofsky 1972) for a structured landscape (see also Sect. 2.4.1), including e.g. wake-producing obstacles such as hedges or lines of trees (see Fig. 6.3). However, such parameters are seldom available for surfaces that are being studied, leaving the researcher to determine a mean roughness length through aggregation for individual surface classes. The authors remind the reader to be aware that a simple parameter aggregation (see Sect. 2.4) can only be provided if the roughness lengths of the different surfaces are of similar orders of magnitude.

Roughness lengths of different surface types are available in most of the textbooks with reference to a British standard (ESDU 1972). These data, together with other classifications, are given in Table 2.1. Another popular roughness length classification has been published in the European Wind Atlas (Troen and Peterson 1989), which was developed for wind energy applications and as such applies mainly to open terrain (see Table 2.15). The Wind Atlas classification distinguishes only between four general roughness classes and was developed for landscapes with high wind energy potential. Larger forested areas are assigned a roughness length value of 0.4 m—a very low estimation compared to other classification schemes and measured values—reflecting the fact that wind turbines are usually placed far away from large forests. The reader is thus advised to use different roughness length classifications spanning a greater range of z_0 values for landscapes dominated by forests. As a third commonly used classification scheme, the roughness length values proposed by Fiedler, cited in Hasager and Jensen

(1999), are based on micrometeorological field observations made in various land cover types within the region of the Upper Rhine Valley, Germany. The fourth classification scheme cited here (Wieringa 1992) compiles quality-proofed roughness length measurements from several hundred original publications. Finally, the last roughness length classification developed by Davenport et al. (2000) presents effective roughness lengths, assuming a more heterogeneous characteristic of the given land cover types as in the effective values presented by Fiedler and Panofsky (1972). Therefore, their values may be slightly larger than the presented in the other four schemes (Wieringa 1992).

According to a study by Reithmaier et al. (2006), it is critically important to ensure that the dominating land cover type in the area surrounding the tower be correctly classified. Therefore, for studies in predominantly forested areas, we recommend using the classification scheme of Wieringa (1992). In studies over a more heterogeneous landscape, a classification providing effective roughness lengths should be preferred (Davenport et al. 2000). A second criterion to take into account for the choice of a suitable roughness length classification is the footprint model itself. Some footprint models become numerically unstable for very high roughness length values, and there is usually a maximum threshold for the ratio of measuring height z_m and the roughness length z_0. For example, the analytic model by Schmid (1997) cannot be applied for ratios of $z_m/z_0 < 12$. Other models are less sensitive to this ratio, like e.g. the algorithm proposed by Kormann and Meixner (2001) that uses measured wind velocity and friction velocity instead of roughness length as input. Since the roughness length can be calculated from wind speed and friction velocity (e.g. Eq. 2.16), this approach is basically another version of calculating an effective roughness length.

The use of effective roughness lengths can only replace a full-scale flux aggregation scheme when the chosen effective roughness length is valid over the footprint area. Based on readily available classification schemes e.g. Davenport et al. (2000), this condition is seldom fulfilled. Furthermore, in the paper by Fiedler and Panofsky (1972), large scale aggregated values are given only for flat landscapes (0.42 m), landscapes with small hills (0.99 m), and for hilly regions (1.42 m). Therefore, an area averaging roughness lengths is generally necessary in footprint models requiring homogeneous surface properties. Flux aggregation tools such as the one proposed by Hasager and Jensen (1999) overcome this problem by averaging the friction instead of the roughness length itself. Note that the roughness length of a certain natural surface technically also depends on influence of the wind field on the surface; however, such effects should be negligible within this context.

6.2.2 Remote-Sensing Data

The remote-sensing approach is the method of choice to analyze and describe land cover structure at a field site. Remote sensing databases have first been used for

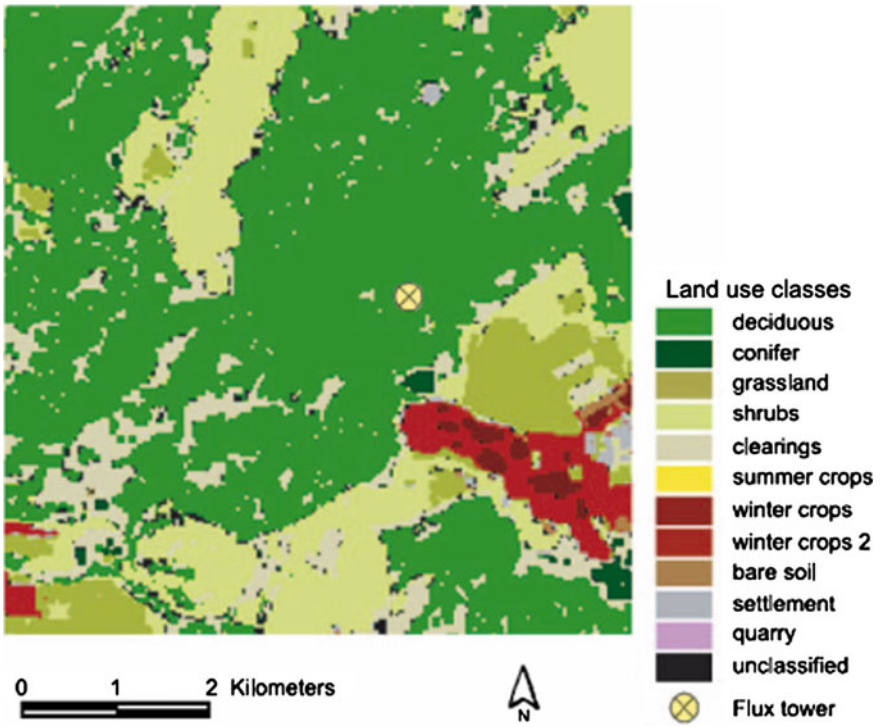

Fig. 6.4 Land use map of the FLUXNET site Hainich DE-Hai based on remote sensing data from Landsat ETM+ with 30 m resolution (Reithmaier et al. 2006)

this purpose during large-scale experiments like FIFE (Sellers et al. 1988) or BOREAS (Sellers et al. 1997) in the 1980s and 1990s. Satellite techniques are a valuable tool to identify surface patterns for footprint analyses at very high resolution of 25 × 25 m^2 or smaller (Fig. 6.4). Resolution and sampling frequency vary by satellite type and employed spectral channels. An overview over available satellite types is given in Table 6.3. Because of the presence of clouds satellites providing high-resolution imagery pass over specific regions only at low temporal resolution. Thus, in many locations, images can only be updated at seasonal intervals, while changes in land use taking place over shorter timescales. Important effects such as e.g. crop harvest, leaf development and leaf fall in deciduous forests and agricultural crops, go undetected.

Satellite remote sensing spectral images have to be corrected to account the atmospheric influence, particularly in the case when more than one image is used to classify the land use. If only one image is available, uncorrected images can be used (Song et al. 2001).

Table 6.3 Remote sensing systems technical specifications

Satellite	Landsat 7 (ETM+)	ASTER	IKONOS	MODIS
Orbital period	16 days	16 days	14 days	Daily
Panchromatic	15 × 15 m^2	–	0.85 × 0.85 m^2	
Multispectral	30 × 30 m^2	15 × 15 m^2	4 × 4 m^2	(1,2) 250 × 250 m^2 (3–7) 500 × 500 m^2
Thermal	60 × 60 m^2	90 × 90 m^2		
Band (multispectral)				
1	450–520 nm		450–520 nm	(3) 459–479 nm
2	520–600 nm	(B1) 520–600 nm	520–600 nm	(4) 545–565 nm
3 (red)	630–690 nm	(B2) 630–690 nm	630–690 nm	(1) 620–670 nm
4 (NIR)	760–900 nm	(B3) 760–860 nm[a]	760–900 nm	(2) 841–876 nm
5 (SWIR)	1,550–1,730 nm	(B4) 1,600–1,700 nm		(5) 1,230–1,250 nm (6) 1,628–1,652 nm
7 (SWIR)	2,080–2,350 nm	(B5) 2,185–2,225 nm		(7) 2,105–2,155 nm
Band (thermal)				
6	10.4–12.5 μm	(B14) 10.25–10.95 μm (B15) 10.95–11.65 μm		

[a] Nadir, B4: backward scan

The most common spectral index to detect spatial and temporal variability of biomass, and therefore evaluate the distribution of land-cover types, is the Normalized Difference Vegetation Index (NDVI). NDVI is based on the difference of the red reflectance (band 3, Landsat) and the NIR reflectance (band 4):

$$NDVI = \frac{NIR - red}{NIR + red} \tag{6.1}$$

Differences in red and NIR wavelengths are mainly caused by the canopy architecture of green vegetation. Using this contrast of reflectance and absorption, the amount of vegetation present on the surface can be evaluated. It is also necessary to calculate the ratio of the spectral bands 7 und 5 to identify from the reflectance rocks and soils (Richards 1993). However, these bands are not available using IKONOS data. The latter provides high resolution information of canopy cover. This information was successfully used by Kim et al. (2006) to determine the crown cover of a forest.

While the NDVI is chlorophyll sensitive the Enhanced Vegetation Index (EVI) represents better the canopy structure including the leaf area index (Huete et al. 2002):

Table 6.4 Contribution of different land use types in percentage in the area of the FLUXNET site Waldstein-Weidenbrunnen (DE-Bay, 36.18 km^2) for different resolutions of remote sensing images (Reithmaier et al. 2006)

Resolution	15 (m)	30 (m)	50 (m)	75 (m)	100 (m)
Conifer	61.1	61.1	61.0	61.2	61.1
Clearings	12.3	12.2	12.1	12.0	11.9
Grassland	5.6	5.6	5.5	5.7	5.6
Summer crops	6.5	6.5	6.6	6.6	6.7
Winter crops	6.2	6.2	6.4	6.3	6.6
Settlements	4.8	4.9	4.9	5.0	5.0
Quarry	0.3	0.3	0.3	0.4	0.4
Unclassified	3.2	3.2	3.1	3.0	2.7

Note, due to a storm event in 2007 the area of clearings is now much larger as given in this table (Foken et al. 2012)

$$EVI = G\frac{NIR - red}{NIR + C1 \cdot red - C2 \cdot blue + L} \tag{6.2}$$

The factors are C1 = 6, C2 = 7.5, and the gain factor G = 2.5 and L = 1. For the case of the absence of the blue band (MODIS channel 3) the factors can be changed to C1 = 2.4, C2 = 0.

To convert remote sensing spectral bands into land cover types, standard classifiers like e.g. the maximum likelihood classifier (Richards 1993) can be employed (Fig. 6.4). The accuracy of the adopted classifier needs to be determined based on different statistical tests (Smits et al. 1999), as well as in situ comparisons over a test area (ground truthing).

Reithmaier et al. (2006) tested the influence of map resolution on the ability of footprint models to detect the influence of disturbance on eddy-covariance measurements. In a first analysis, they tested how different map resolutions affected the simulated distribution of the land-use types in the larger area. They found that, at their test site, the resolution of the images had no impact on the frequency of the land-use type (see Table 6.4), and the contribution of certain land-cover classes did not shift significantly between map versions. However, in the same study Reithmaier et al. (2006) also showed that the higher level of details maintained in the land cover structure of a remote sensing map can significantly shift footprint results as compared to the use of a very low resolution map (e.g. a 100 × 100 m^2 map read out from topographical maps). As shown in Fig. 6.5, the flux contribution from the target area (here: conifer forest) is much larger using the land use classification of a topographic map than of those by remote sensing data. This shift is caused by removing small-scale heterogeneities such as clearings by applying of a majority filter in coarser maps. Though these areas may appear small and insignificant, their cumulative effect can be important in the average land-use classification. Remote sensing identifies these areas, and thus can provide a more realistic picture of the flux contributions.

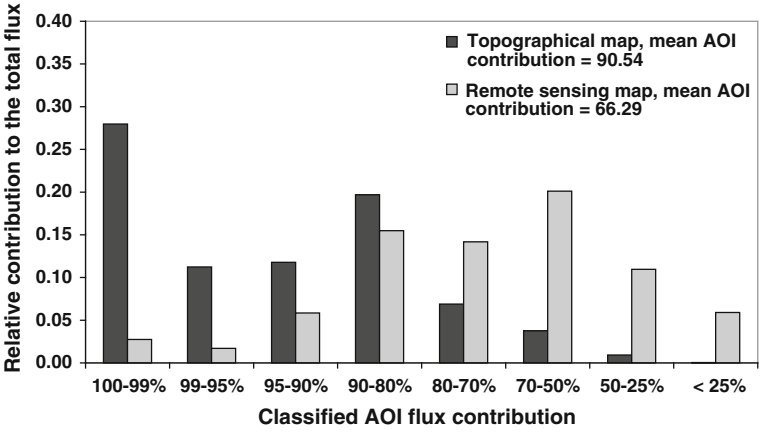

Fig. 6.5 Relative flux contribution of the area of interest (AOI, conifer forest) to the measured flux at the FLUXNET site Waldstein-Weidenbrunnen (DE-Bay) of both, the remote sensing data set (resolution 15 × 15 m^2) and the topographical map (resolution 100 × 100 m^2) according to Reithmaier et al. (2006)

In conclusion, the resolution of land-use classification should be high especially when landscapes are characterized by small-scale heterogeneities. This can be most effectively realized with the help of remote sensing data. Over more homogeneous land covers and footprint calculations for stable stratification with associated larger footprint areas, low resolution maps are acceptable.

Remote sensing data for land use classification were used by several authors (Hasager et al. 2003; Rebmann et al. 2005; Reithmaier et al. 2006). The main principle combined land-use classifications that use roughness lengths and to use averaging procedures for the roughness lengths within the footprint area.

Kim et al. (2006) accumulated the Normalized Difference Vegetation Index (NDVI) over the footprint area by weighting the NDVI of each grid cell with its footprint function f_i:

$$NDVI_f = \sum_{i=1}^{N} (f_i \cdot NDVI_i) \tag{6.4}$$

In the same way, they studied the crown closure or stand density. This is defined as the percentage of the ground covered by vertically projected crown in a stand. They used the IKONOS panchromatic band with 1 m resolution to detect the distribution of trees. This is comparable with the aggregation schema used by Göckede et al. (2004, 2006) and provided in Sect. 6.3.

6.3 Coupling Footprint Results with Surface Information

Procedures to link surface information to footprint areas have been proposed for a matrix of roughness lengths by Grimmond et al. (1998) and later applied by Göckede et al. (2004) for use in footprint investigations. According to Göckede et al. (2004), the source-weight function has to be calculated for each individual step of the time series (e.g. 30 min intervals), and projected onto the land cover matrix according to actual meteorological conditions like wind velocity, stability, or other parameters influencing the output of the type of footprint model chosen. Weighting factors ranging from zero to one reproducing the source weight function were assigned to all matrix cells lying within the concentric 10–90 % isopleths produced by the footprint model, while all matrix cells outside this area were labelled with a weighting factor of zero (Fig. 6.1). Subsequently, for each matrix cell, land-cover information (up to N different land cover types) read out from the matrix was multiplied by the assigned weighting factor (for example, footprint function of the effect level f^P, Eq. 2.94 in combination with Eq. 3.5), and the final roughness length z_0 for the specific measurement was determined as the linear average of these products:

$$z_o = \sum_{i=1}^{N} \left(f_i^P \cdot z_{0i} \right) \tag{6.4}$$

If land cover characteristic such as the roughness length is also an input parameter in the footprint model, the entire process should be repeated iteratively with computed roughness lengths as the new input value, until the difference between input and output roughness length falls below a user-defined threshold. The first model runs for each 30 min-measurements has to be performed with an approximate value for the roughness length. Usually, no more than three iterations are necessary to reach the final roughness length. Because this roughness length was determined as a linear mean, the algorithms performed a parameter aggregation, while roughness length values provided by the matrix are prepared using a non-linear flux aggregation approach (see Sect. 2.4.2). From the physical standpoint, a flux aggregation is better suited method. This approach was used successfully by Göckede et al. (2006) and showed to differ from the simple approach. It can be concluded that the accuracy of the results was significantly improved.

References

Davenport AG, Grimmond CSB, Oke TR, Wieringa J (2000) Estimating the roughness of cities and sheltered country. In: 12th Conference on Applied Climatology, Ashville, NC2000. American Meteorological Society, pp. 96–99

ESDU (1972) Characteristics of wind speed in the lowest layers of the atmosphere near the ground: strong winds. Engineering Sciences Data Unit, London, 35 pp

Fiedler F, Panofsky HA (1972) The geostrophic drag coefficient and the 'effective' roughness length. Quart J Roy Meteorol Soc 98:213–220

Foken T et al (2012) Coupling processes and exchange of energy and reactive and non-reactive trace gases at a forest site—results of the EGER experiment. Atmos Chem Phys 12:1923–1950

Göckede M, Rebmann C, Foken T (2004) A combination of quality assessment tools for eddy covariance measurements with footprint modelling for the characterisation of complex sites. Agric Forest Meteorol 127:175–188

Göckede M, Markkanen T, Hasager CB, Foken T (2006) Update of a footprint-based approach for the characterisation of complex measuring sites. Boundary-Layer Meteorol 118:635–655

Grimmond CSB, King TS, Roth M, Oke TR (1998) Aerodynamic roughness of urban areas derived from wind observations. Boundary-Layer Meteorol 89:1–24

Hasager CB, Jensen NO (1999) Surface-flux aggregation in heterogeneous terrain. Quart J Roy Meteorol Soc 125:2075–2102

Hasager CB, Nielsen NW, Jensen NO, Boegh E, Christensen JH, Dellwik E, Soegaard H (2003) Effective roughness calculated from satellite-derived land cover maps and hedge-information used in a weather forecasting model. Boundary-Layer Meteorol 109:227–254

Huete A, Didan K, Miura T, Rodriguez EP, Gao X, Ferreira LG (2002) Overview of the radiometric and biophysical performance of the MODIS vegetation indices. Remote Sens Environ 83:195–213

Kim J, Guo Q, Baldocchi DD, Leclerc MY, Xu L, Schmid HP (2006) Upscaling fluxes from tower to landscape: overlaying flux footprints on high resolution (IKONOS) images of vegetation cover. Agric Forest Meteorol 136:132–146

Kormann R, Meixner FX (2001) An analytical footprint model for non-neutral stratification. Boundary-Layer Meteorol 99:207–224

Rebmann C et al (2005) Quality analysis applied on eddy covariance measurements at complex forest sites using footprint modelling. Theor Appl Climat 80:121–141

Reithmaier LM, Göckede M, Markkanen T, Knohl A, Churkina G, Rebmann C, Buchmann N, Foken T (2006) Use of remotely sensed land use classification for a better evaluation of micrometeorological flux measurement sites. Theor Appl Climat 84:219–233

Richards JA (1993) Remote sensing digital image analyse—An introduction. Springer, Berlin 340 pp

Schmid HP (1997) Experimental design for flux measurements: matching scales of observations and fluxes. Agric Forest Meteorol 87:179–200

Sellers PJ, Hall FG, Asrar G, Strebel DE, Murphy RE (1988) The first ISLSCP field experiment (FIFE). Bull Amer Meteorol Soc 69:22–27

Sellers PJ et al (1997) BOREAS in 1997: Experiment overview, scientific results, and future directions. J Geophys Res 102:28731–28769

Smits PC, Dellepiane SG, Schowengerdt R (1999) Quality assesment of image classification algorithms for landcover mapping: a review and a proposal for a cost-based approach. Int J Remote Sens 20:1461–1486

Song C, Woodcock CE, Seto KC, Lenney MP, MacOmber SA (2001) Classification and change detection using Landsat TM data: when and how to correct atmospheric effects? Remote Sens Environ 75:230–244

Troen I, Peterson EW (1989) European Wind Atlas. Risø National Laboratory, Roskilde 656 pp

Wieringa J (1992) Updating the Davenport roughness classification. J Wind Eng Ind Aerodyn 41:357–368